Оптический журнал

Биомедицинская оптика

Classification of maize leaf diseases based on hyperspectral imaging technology

© 2020 Jing Xu*, Teng Miao*, Yuncheng Zhou*, Yang Xiao*, Hanbing Deng*, Ping Song*, Kai Song*, **

*College of Information and Electrical Engineering, Shenyang Agricultural University, Shenyang, 110866, P. R. China

**Shenyang Ligong University, Shenyang, 110159, P. R. China

E-mail: xujingsyau@163.com, songsylu@163.com

Submitted 04.01.2019

DOI:10.17586/1023-5086-2020-87-04-28-35

Curvularia lunata and aureobasidium zeae are the main leaf diseases of maize in Northeast China. Meanwhile, the two diseases are similar and difficult to distinguish. In order to diagnose diseases correctly, a diagnostic method based on hyperspectral imaging technology for curvularia lunata and aureobasidium zeae was proposed. The experimental leaves were inoculated in vivo, and hyperspectral imaging system was used to collect the hyperspectral image data of the leaves of the Curvularia lunata, the leaves of aureobasidium zeae and the normal leaves at the near-infrared band. By analyzing the spectral characteristics of chlorotic spots and normal leaves, it is found that there is a significant difference in spectral information between chlorotic spots and normal leaves. Then, by means of confidence interval estimation and significance test, the characteristic bands of curvularia lunata and aureobasidium zeae can be distinguished. Finally, the classification model of support vector machine is established based on the characteristic bands. The results show that the 10 characteristic bands of 412.7 nm, 416.3 nm, 421.2 nm, 465.1 nm, 484.8 nm, 580.9 nm, 615 nm, 640.5 nm, 676.2 nm, 880.8 nm can be used to distinguish between curvularia lunata and aureobasidium zeae spectral characteristics of the disease, and the support vector machine classification model established by the above band is used for 288 samples. The accuracy rate was 96.7%. These results provide a theoretical basis and technical method for rapid and non-destructive diagnosis of curvularia lunata and aureobasidium zeae.

Keywords: *curvularia lunata, aureobasidium zeae, confidence interval estimation, significance test, hyperspectral imaging technology, support vector machine.*

OCIS codes: *100.4145, 150.1135, 100.0100, 300.6280, 300.6550, 000.5490.*

Классификация заболеваний листьев маиса с использованием технологии гиперспектральных изображений

© 2020 г. Jing Xu, Teng Miao, Yuncheng Zhou, Yang Xiao, Hanbing Deng, Ping Song, Kai Song

Curvularia lunata и aureobasidium zeae являются основными грибковыми заболеваниями листьев маиса в северо-восточном Китае. Эти заболевания очень схожи и трудноразличимы. Предложен основанный на технологии гиперспектральных изображений способ их коррект-

ной диагностики. Листья, поражённые Curvularia lunata, aureobasidium zeae, а также здоровые листья маиса подвергались инокуляции in vivo, а затем исследовались с помощью гиперспектральной аппаратуры в ближнем инфракрасном диапазоне. Путём анализа хлоротических пятен было установлено, что существует существенное отличие гиперспектральных характеристик повреждённых и неповреждённых листьев. Далее, используя средние доверительные интервалы и критерии значимости, выделялись характеристические спектральные полосы, позволяющие различить поражения curvularia lunata и aureobasidium zeae. Наконец, на основе данных об этих полосах построена классификационная модель с использованием метода опорных векторов. Показано, на основе анализа 288 изображений образцов, что с использованием разработанной классификационной модели возможно выполнить указанное различение на основе десяти следующих характеристичеких полос: 412,7 нм, 416,3 нм, 421,2 нм, 465,1 нм, 484,8 нм, 580,9 нм, 615 нм, 640,5 нм, 676,2 нм, 880,8 нм. Точность различения составила 96,7%. Таким образом, заложен теоретический базис и предложен метод технический реализации быстрого неконтактного диагностирования curvularia lunata и aureo basidium zeae.

Ключевые слова: *curvularia lunata, aureobasidium zeae, оценка доверительного интервала, оценка значимости, технология гиперспектральных изображений, метод опорных векторов.*

INTRODUCTION

Maize is one of the most widely distributed grain crops in the world. The acreage of maize is the third largest in the world after wheat and rice. And maize is the main food crops in China. And it is also the feed and raw materials of industry. The area of the acreage of maize in China is just after America. In China, the area of maize is divided into three parts on the basis of natural condition. The first part is northern spring maize region, covering Liaoning, Jilin, Heilongjiang, Inner Mongolia, Ningxia, Shanxi, Hebei and so on. This region takes up about 30% of the grain-sown area of maize in China. The second part is summer sowing maize in Huang Huai Plain, including Shandong, Henan, Hebei and South Shanxi. This region takes up about 40% of the grain-sown area of maize in China. The third part is maize region of Hilly and hilly regions in Southwest China, including Sichuan, Yunnan, Guizhou and Guangxi, Hunan, Hubei and other provinces. This region occupies 20% of the grain-sown area of maize in China. In fact maize is planted almost all over the country except some alpine area in the north of China. With the expansion of the area of maize growing and the effect of climate and environment, maize diseases have become an important factor that limit the high and stable yields of maize.

According to different parts of the disease, the maize diseases are generally divided into leaf diseases, ear diseases, stem diseases and root diseases. The common leaf diseases are Northern Leaf Blight, Maize Southern Leaf Blight, Gray Leaf Spot of Maize, Curvularia Lunata and Aureobasidium Zeae.

Curvularia lunata, also called Draft Eye Spot Disease, is a leaf disease that caused by Curvularia lunata (Wakker) Boedijin in China. It's a critical disease spread among Northeast China and North China maize production area in the middle and late 1990s [1]. And it's also a catastrophic disease after Northern Leaf Blight and Maize Southern Leaf Blight [2]. Aureobasidium Zeae [3] is also called eye spot disease. The pathogenic bacteria is Aureobasidium zeae (Narita et Hiratsuka) Dingley. In recent years, aureobasidium zeae is mainly distributed in Liaoning, Jilin, Heilongjiang, Yunnan and other provinces. And this disease has become the main disease in some parts of Liaoning [4]. Aureobasidium zeae is often happening with curvularia lunata, maize will be killed in the place where the maize has been critically infected this disease.

When the disease happens, it is effective to stop it from spreading if we recognize accurately what the disease is and prescribe medicine according to the disease. Nowadays, the recognition of curvularia lunata and aureobasidium zeae depends mainly on manual work according to experience. However, this kind of recognition has low efficiency and requires high quality of man. The two diseases have similar disease spot, especially in the early stage of the dis-

ease. Man can judge these diseases mistakenly so that it will reduce the accuracy of recognition and delay the best time of applying medicine. Therefore, when the disease occurs, we can prevent it from further damaging if we recognize the disease rapidly and accurately. And it plays an important part in reducing medicine, controlling pollution and increasing the quality of crops.

Combining imaging technology with spectral technology, hyperspectral imaging technology makes meticulous division in terms of spectral dimension, gets the image of continuous and narrow band resolution, and can obtain the spectral and image information of the object at the same time. Presently hyperspectral technology has been applied to soil and crop monitoring [5–11] and grain quality analysis, such as cereals, oilseeds, fruits and vegetables [12–17]. In recent years, some scholars have applied hyperspectral imaging technology to the detection of plant diseases and insect pests, and have made certain progress. In laboratory conditions, neural network and principal component analysis were used to discriminate and classify the infection levels of different fungi in Rice Panicles by Liu and others based on hyperspectral imaging technology [18]. The spectral response characteristics of Rice Panicles were analyzed based on the hyperspectral data of Rice Panicles collected in the 350–2500 nm wavelength range. The main components of different spectral processing methods are obtained by PCA, and the learning vector quantization neural network classifier is used to classify different levels of infection. The total accuracy of LVQ and PCA obtained from the reflection spectrum from the two derivative of the test data set has reached 100%. Research results showed that hyperspectral data could be used to identify the infection level of different panicle fungi in Rice under laboratory conditions. Jones and others [19] have determined the degree of bacterial leaf spot disease in tomato leaves with the help of UV, visible light and near-infrared reflectance spectroscopy, identified the characteristic wavelengths by chemometric method and established the prediction model. Several important regional wavelengths were determined by partial least square regression, correlation coefficient spectrum analysis and stepwise multiple linear regression, and the prediction model of disease degree based on absorption spectrum was established. As the result showed, the result is the best of the model of partial least squares regression based on B value, in which the determining coefficient is 0.82 and the root mean square error is 4.9%, manifesting that it is feasible to detect tomato bacterial leaf spot by spectral technique. Zhang and others [20] measured the hyperspectral reflectance of winter wheat leaves of normal and powdery mildew infection under laboratory conditions, and extracted 32 spectral characteristics. Then they established multiple linear regression and partial least two multiplying regression model by correlation analysis and independent t test related to the severity of the disease to predict the severity of the powdery mildew. And the results showed that the extracted spectral characteristics of the ion showed a significant response to powdery mildew. The partial least squares regression model was better than that of the multiple linear regression when the spectral characteristic method was used to identify the severity of the disease. Feng and others [21] extracted the leaf blast of rice infected leaves and canopy image data, based on the multi spectral imaging technology and established a detection model for the analysis of the disease of rice leaf blast. The results showed that the recognition rate of leaf plague with green, red and near infrared three band channels is high. It can discover the occurrence of disease and display the location of the disease spot in time. The classification model of rice leaf blast is established, the accuracy rate of rice seedling plague recognition is 98% and the recognition rate of leaf blast reaches 90%. It can achieve rapid and non-destructive detection of rice leaf blast. The recognition rate of leaf plague is high with the help of multispectral imaging technology covering such three band channels as green, red and near infrared, and it could detect the occurrence of disease and display the location of disease spots in time. The established disease grading model of rice leaf blast could promote the accuracy of the identification of rice seedling plague to 98% and that of leaf plague to 90%, realizing the rapid and nondestructive testing of rice leaf blast. Sun and others [22] proposed a method of real-time identification of barley scab based on multi spectral image, extracted the image color statistical characteristics using threshold segmentation and morphological processing algorithm to re-

move the image background and interference information and analyzed the pattern feature by partial least squares. The disease recognition model was established based on support vector machine and the accuracy of the identification of disease reached 93.9%. Based on the experiment of powdery mildew inoculation on the field and potted wheat, Feng Wei and others [23] determined the group spectrum and chlorophyll density of different growth period under the disease stress, analyzed the relationship between the spectral reflectance of the group, the characteristic parameters of the traditional spectrum and the chlorophyll density of the canopy, and then established the estimation model of the chlorophyll density of the disease. As the results showed, with the aggravation of the disease, chlorophyll content decreased, and there was the most significant correlation between the chlorophyll density of disease canopy and the first order differential of the red light (600–630 nm), the red edge (690–718 nm) and the red border length (718–756 nm). The normalized angle index was regarded as a reliable index for estimating the chlorophyll density of the disease wheat canopy. Xu and others [24] proposed an early identification of curvularia lunata method based on hyperspectral imaging technology. The experiment leaves are in vitro inoculation, at 11 time points after inoculation (2, 4, 6, 8, 12, 24, 32, 40, 48, 60, 72 hours respectively), collect hyperspectral images in the visible and near infrared bands of normal leaves and inoculation disease leaves respectively by hyperspectral imaging system. Based on mixed distance method, find that the best bands of identification curvularia lunata are 465.1 nm, 550.7 nm, 681.4 nm. As the results provided research foundation for detecting the Curvularia lunata (Wakker) Boedijin in early time and provided a new idea for detecting the maize disease in its early stage.

The study was carried out on the maize leaves inoculated curvularia lunata and aureobasidium zeae. In the study, the hyperspectral image information was obtained from the infected leaves, and the qualitative analysis method was used to construct the diagnosis system of curvularia lunata and aureobasidium zeae, to provide a new method for automatic, rapid and nondestructive testing of maize diseases.

1. MATERIALS AND METHODS

1.1. Experiment Materials

Maize leaves were tested in this study. In order to avoid the infection in the process of natural growth in the outside field, the disease resistant variety ZengYu 1572 were selected for the test, they were provided by Special Maize Institute of Shenyang Agricultural University. The tested strains were curvularia lunata strain CX-3,aureobasidium zeae strain CLNKZ-1 provided by Laboratory of Molecular and Physiological Plant Pathology of Shenyang Agricultural University. Maize samples were sown in the maize experimental field at the Teaching and Scientific Research Base of Shenyang Agricultural University in June 10, 2017. There are 10 grains per line, and 30 grains per row, with 60 cm in row spacing, and 30 cm in plant spacing to ensure that each plant be in good sunshine, good ventilation, and the temperature and humidity be under the same environment. In August 7, 2017, the maize grew to the jointing stage, and the test was carried out after the maize was inoculated against curvularia lunata and aureobasidium zeae.

Inoculation was carried out in vivo, and the similar position was set at the eighth leaves of each plant to make the infection process as similar as possible. Among them, there were 120 plants inoculated curvularia lunata, the other 120 plants inoculated aureobasidium zeae. Only 60 plants were set as the control group with no inoculation. When the inoculation was conducted, the bacteria cake was cut with a 6-mm-bore puncher that was disinfected from the grains having been cultivated for 10 days, and the mycelium was attached to the surface of the maize leaf and marked with the marker pen. After inoculation, the leaves were artificially recharged every day with a small watering pot. Three days later, leaf spots appeared on the leaves that were inoculated curvularia lunata, and about ten days later, leaf spots also appeared one after another on the leaves that were inoculated aureobasidium zeae. Then hyperspectral image data of the spotted leaves were collected.

1.2. Hyperspectral Imaging System

Hyperspectral image data were collected by hyperspectral image system in the study, as shown in Fig. 1. And the system includes a high

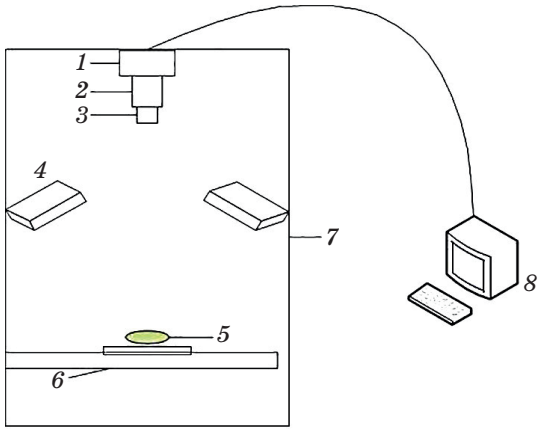

Fig. 1. Hyperspectral imaging system: camera *1*, spectrometer *2*, lens *3*, light source *4*, sample *5*, displacement platform *6*, black box *7*, computer *8*.

spectrometer (ImSpector V10E), CCD camera (IMPERX IGV-B1410M), halogen light source (IT 3900, 1500W), spotlight, mobile platform and computer. The collected spectral wavelength ranges from 400 to 1000 nm, covering 512 bands and the spectral resolution is 2.8 nm. In order to improve the acquisition accuracy and avoid the influence of ambient light, the whole system was placed in a closed black box.

1.3. Hyperspectral Image Collection

In order to ensure the accuracy of the collected spectral information, the leaves of maize were tested in vitro. 1 leaf sample was put on the black carrier table each time, and 300 maize leaf samples were collected altogether, among which there were 120 leaves with chlorotic spots of curvularia lunata, 120 leaves with chlorotic spots of aureobasidium zeae and 60 leaves with no inoculation. Before collecting hyperspectral image data, it is necessary to adjust the exposure time of the hyperspectral camera and the moving speed of the platform according to the height of the lens, the focal length and the brightness of the light source, so as to ensure the clarity of the image. After repeated modification, the final exposure time was set at 8.5 ms, the distance between objects was 430 mm, and the speed of the displacement table was 2.85 mm/s. When the data were collected, the maize leaves moved at a constant speed with the platform, and the hyperspectral camera and the image spectrometer got the spectral information of each pixel at each wavelength and the image data at each band.

2. DATA PROCESSING AND ANALYSIS

The data collection software is spectral-image by ISUZU OPTICS, the ENVI5.1 (Research System Inc., Boulder, Colo., USA), Matlab2012a (The MathWorks Inc., Natick, USA), Excel2013 (Microsoft, USA) and Microsoft Visual Studio 2013 are used in data processing.

2.1. Black and White Calibration of Spectral Data

In order to eliminate the influence of the image noise and dark current in the weak distribution of the light intensity, the reflection spectrum of the image should be corrected before the high spectral image collection, and the correction method is black and white calibration. Firstly, we scanned the white board, which has a high reflectivity and extracted the white labelled image R_{white} whose reflectivity is 100%. Secondly cover the lens cap and collect the full black calibration image R_{dark} with a reflectance of 0. Thirdly the maize leaves were placed on the loading stage to collect the spectral images R_{sample} of the samples. Finally the corrected reflectivity R at band i was calculated according to Formula (1).

$$R(i) = \frac{R_{\text{sample}}(i) - R_{\text{dark}}(i)}{R_{\text{white}}(i) - R_{\text{dark}}(i)}. \quad (1)$$

2.2. Selection of Regions of Interest and Characteristic Bands in Maize Leaves

From the leaf samples collected by hyperspectral imaging system, and image data of each band from 400 to 1000 nm, 360 interest regions were respectively selected from the 120 leaves with chlorotic spots of curvularia lunata, from the 120 leaves with chlorotic spots of aureobasidium zeae, and from the normal part of the leaves with no inoculation. For the spotted leaves, the spotted part is selected as interest region, and for the normal part, the pixel of 20×20 was selected as the interest region.

The mean spectra of the selected regions of interest of three maize leaf samples were calculated, and their spectral curves are shown in Fig. 2. From Fig. 2, the reflectance of the chlorotic spots of curvularia lunata and chlorotic spots of aureobasidium zeae were higher than that of normal leaves in 400–730 nm interval. And in the 790–1000 nm interval, the reflec-

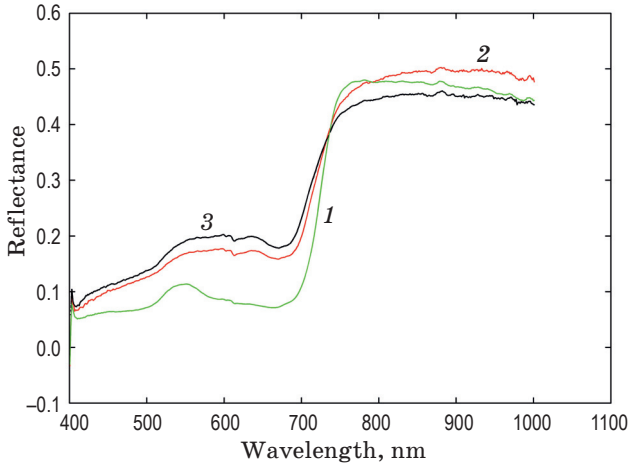

Fig. 2. Reflectance spectrum of normal leaves (*1*), chlorotic spots of Curvularia lunata (*2*), and chlorotic spots of Aureobasidium zeae (*3*).

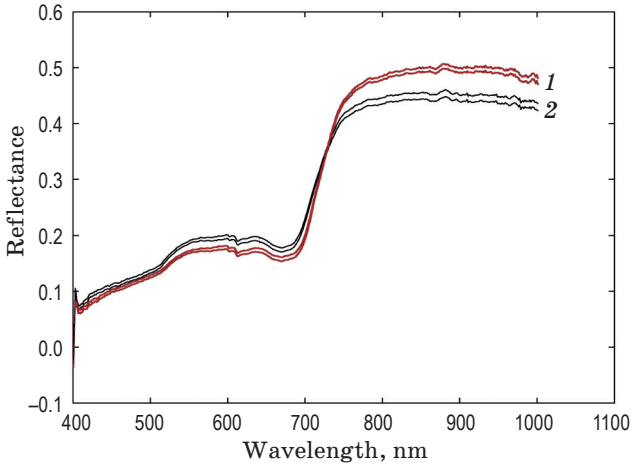

Fig. 3. The 95% confidence interval for mean of spectrum of chlorotic spots of Curvularia lunata (*1*), and chlorotic spots of Aureobasidium zeae (*2*).

tance of the chlorotic spots of curvularia lunata was the highest, followed by the normal leaves, and chlorotic spots of aureobasidium zeae was the lowest.

2.2.1. Statistical Inference

The interval estimation of parameters is a method based on a certain theoretical distribution. It is known from the central limit theorem of statistics and the law of large numbers that the sample average is approximately normal distribution, if the sample is a large sample ($n > 30$), whether it is a normal distribution or not. The mean value is the main observation index of the trend of the data set. The mean confidence interval estimation is based on the error of the mean point estimate and the sampling standard, and it does give an interval range of the overall parameters at a certain confidence level. In the acquisition of spectral data, due to the effect of some factors, the data collected will contain random errors, and the mean confidence interval estimation limits the sampling error to a certain range. When the degree of confidence $P = 1 - \alpha$, the confidence interval was shown as Formula (2).

$$P(\bar{x}_i - u_a\sigma_{\bar{xi}} \le u_i \le \bar{x}_i + u_a\sigma_{\bar{xi}}) = 1 - a. \quad \textbf{(2)}$$

In Formula (2), $\bar{x}_i$ is the mean value of the spectral reflectance in the Band i, $\sigma_{\bar{xi}}$ is total standard deviation, and α represents the significant level. For band i with a range of 400–1000 nm, the confidence interval of all bands constitutes the confidence interval band of spectral reflectance mean.

Hyperspectral data have many bands and narrow band spacing, so the hyperspectral data are large and there are lots of redundant data. For the selection of the feature band, N bands were selected the ($N < M$) from the original M bands to achieve the purpose of representing the information of the M bands with the N bands, so as to reduce the dimension of the spatial data. Use the confidence interval to select the feature band of the spectrum, as shown in Fig. 3. With the overlap of the 95% confidence intervals of the two disease spectrum curves removed in Fig. 3, it could be set as the feature band selection area that was used to make a distinguish between curvularia lunata and aureobasidium zeae. Through comparison and analysis, 420–700 nm and 780–1000 nm were selected as the best band selection area.

2.2.2. Significance Test

The adjacent bands of hyperspectral image data have strong correlation. In order to better detect disease and reduce redundant data, it is necessary to further extract the most separable band in the best band selection area. Based on the overall theoretical distribution and the principle of small probability, the significance test put forward two opposing hypotheses to the unknown or incomplete knowledge. And then, the actual results of the sample were calculated to make the assumption that the hypothesis

should be accepted in a certain probability. The difference in the corresponding spectrum of the selection region of curvularia lunata and aureobasidium zeae was judged by the significance test, and the feature bands were further extracted according to the significance of the difference. For the best band selected arranging from 420–700 nm to 780–1000 nm, after a significant test, 9 bands were selected in the visible region, and 1 bands were selected in the near-infrared region, as shown in Table 1, as the feature band of curvularia lunata and aureobasidium zeae.

2.3. Disease Recognition Based on Support Vector Machine Classification Algorithm

Support vector machine (SVM), as a pattern recognition method, is widely used in classification problems and has many unique advantages in solving the problem of pattern recognition, such as nonlinear, high dimension and local minimum. The 10 feature bands selected were made as the attribute value used to distinguish curvularia lunata from aureobasidium zeae, from the 360 samples of curvularia lunata and the same size of aureobasidium zeae, 216 samples were respectively selected as training set samples, and 144 as test set samples. First, the training set and test set were normalized, and then the training set was trained by different kernel functions to get the classification model. Finally, the classification accuracy was obtained by testing the test set according to the classification model. The test results were shown in Table 2.

3. CONCLUSIONS

The study on curvularia lunata and aureobasidium zeae of maize was conducted based on the hyperspectral imaging technology, and the conclusions were drawn as below:

(1) Based on the central limit theorem of statistics and the law of large numbers, a method based on mean confidence interval is proposed to identify the optimal waveband area of lesion. As analysis showed the best band selection area is 420–700 and 780–1000 nm.

(2) The hyperspectral data are large, and the adjacent bands have strong correlation, and there are a lot of redundant data. The best band selection region was further carried out by the significance test, and a more representative feature band was further extracted. Through calculation, such feature bands distinguishing curvularia lunata and aureobasidium zeae were selected as 412.7, 416.3, 421.2, 465.1, 484.8, 580.9, 615, 640.5, 676.2 and 880.8 nm.

(3) Support vector machine classification algorithm was used to classify the 288 spot samples, and the accuracy rate reached 96.7%. The study was made on the spectrum of curvularia lunata and aureobasidium zeae, and the results of it can provide a basis for the identification of maize disease, and provide a new method for automatic, rapid and nondestructive testing of maize diseases.

This research was financially supported by Natural Science Foundation of China (31501217, 31601218, 31701318) and Beijing Municipal Natural Science Foundation (Grant No.4162028).

Table 1. Feature band

No.	Band1	Band2	Band3	Band4	Band5
Wavelength	412.7nm	416.3nm	421.2nm	465.1nm	484.8nm
No.	Band6	Band7	Band8	Band9	Band10
Wavelength	580.9nm	615nm	640.5nm	676.2nm	880.8nm

Table 2. Comparison of SVM between different kernel functions

Kernel functions	Training set	Test set	Correct recognition rate
Linear	432	288	96.7%
Polynomial	432	288	91.6%
Radial basis	432	288	94.3%

REFERENCES

1. *Dai F.C., Wang X.M., Zhu Z.D. et al.* Curvularia leaf spot of maize pathogens and varietal resistance // Acta. Phytopathologica. Sinica. 1998. V. 28(2). P. 123–129.
2. *Chen L.M., Dou S.H., Lv Z.M. et al.* Studies on some epidemic links of maize curvularia leaf spot // J. Maize. Sci. 2006. V. 14(4). P. 148–150, 154.
3. Sun J.Y., Xiao S.Q., Lu Y.Y. Isolation, identification and biological characteristics of Aureobasidium zeae in Liaoning Province // Journal of Plant Protection. 2015. V. 42(6). P. 927–934.
4. *Meng L.M., Su Q.F., Jia J. et al.* Identification of the Pathogen of corn Northern Anthrax and its growth affecting factors // J. Maize. Sci. 2016. V. 24(4). P. 160–165.
5. *Kirshnan P., Alexander J.D., Butler B.J. et al.* Reflectance technique for predicting soil organic matte // Soil sci. soc. Am. J. 1980. V. 44(6). P. 1282–1285.
6. *Dalal R.C., Herry R.J.* Simultanous determination of moisture, organic carbon, and total nitrogen by near infrared reflectance spectrophotometry // Soil sci. soc. Am. J. 1986. V. 50(1). P. 120–123.
7. *Sudduth K.A., Hummel L.W.* Evaluation of reflectance methods for soil organic matter sensing // Transactions of the ASAE. 1991. V. 34(4). P. 1900–1909.
8. *Sudduth K.A., Hummel L.W.* Portable near-infrared spectrophoto meter for rapid soil analysis // Transactions of the ASAE. 1993. V. 36(1). P. 185–193.
9. *Sudduth K.A., Hummel L.W.* Soil organic matter, CEC, an moisture sensing with a portable NIR spectrophotometer // Transactions of the ASAE. 1993. V. 36(6). P. 1571–1582.
10. *Sudduth K.A., Hummel L.W.* Geographic operating range evaluation of a NIR soil sensor // Transactions of the ASAE. 1996. V. 39(5). P. 1599–1604.
11. *Chen P.F., Liu L.Y., Wang J.H. et al.* Real-time analysis of soil N and P with near infrared diffuse reflectance spectroscop // Spectrosc. Spect. Anal. 2008. V. 28(2). P. 295–298.
12. *Lichtenthaler H.K., Langsdorf G., Buschmann C.* Multicolor fluorescence images and fluorescence ratio images of green apples at harvest and during storage // Israel Journal of Plant Sciences. 2012. V. 60(1–2). P. 97–106.
13. *He Y., Li X.L., Shao Y.N.* Discrimination of varieties of apple using near infrared spectra based on principal component analysis and artificial neural network model // Spectrosc. Spect. Anal. 2006. V. 26(5). P. 850–853.
14. *Liu Y.D., Chen X.M., Sun X.D.* Nondestructive measurement of vitamin C in Nanfeng tangerine by visible/near-infrared diffuse reflectance spectroscopy // Spectrosc. Spect. Anal. 2008. V. 28(10). P. 2318–2320.
15. *Yao X., Tian Y.C., Ni J. et al.* Estimation of leaf pigment concentration in rice by near infrared reflectance spectroscopy // Chinese Journal of Analytical Chemistry. 2012. V. 40(4). P. 589–595.
16. *Wang F., Li Y.Y., Peng Y.K. et al.* Determination of Tomato's SSC and TS based on diffuse transmittance spectroscopy // Spectrosc. Spect. Anal. 2016. V. 36(10). P. 3185–3189.
17. *Li H.Q., Sun H., Li M.Z.* Detection of vitamin C content in head cabbage based on visible/near-infrared spectroscopy // Transaction of the CSAE. 2018. V. 34(8). P. 269–275.
18. *Liu Z.Y., Wu H.F., Huang J.F.* Application of neural networks to discriminate fungal infection levels in rice panicles using hyperspectral reflectance and principal components analysis // Computers and Electronics in Agriculture. 2010. V. 72(2). P. 99–106.
19. *Jones C.D., Jones J.B., Lee W.S.* Diagnosis of bacterial spot of tomato using spectral signatures // Computers and Electronics in Agriculture. 2010. V. 74(2). P. 329–335.
20. *Zhang J.C., Pu R.L., Wang J.H. et al.* Detecting powdery mildew of winter wheat using leaf level hyperspectral measurements // Computer and Electronics in Agriculture. 2012. V. 85(1). P. 13–23.
21. *Feng L., Chai R.Y., Sun G.M. et al.* Identification and classification of rice leaf blast based on multi-spectral imaging sensor // Spectrosc. Spect. Anal. 2009. V. 29(10). P. 2730–2733.
22. *Sun G.M., Yang K.S., Zhang C.Q. et al.* Identification of barley scab based on multi-spectral imaging technology // Transaction of the CSAE. 2009. V. 25 (S2). P. 204–207.
23. *Feng W., Wang X.Y., Song X. et al.* Hyperspectral estimation of canopy chlorophyll density in winter wheat under stress of powdery mildew // Transaction of the CSAE. 2013. V. 29(13). P. 114–123.
24. *Xu J., Miao T., Zhou Y.C. et al.* Early identification of Curvularia lunata based on hyperspectral imaging // Journal of Optical Technology. 2018. V. 85(7). P. 432–436.